Development 134, 3677-3689 (2007) doi:10.1242/dev.011577

Phosphorylation of the atypical kinesin Costal2 by the kinase Fused induces the partial disassembly of the Smoothened-Fused-Costal2-Cubitus interruptus complex in Hedgehog signalling

Laurent Ruel, Armel Gallet, Sophie Raisin, Arnaud Truchi, Laurence Staccini-Lavenant, Alexandra Cervantes and Pascal P. Thérond*

The Hedgehog (Hh) family of secreted proteins is involved both in developmental and tumorigenic processes. Although many members of this important pathway are known, the mechanism of Hh signal transduction is still poorly understood. In this study, we analyse the regulation of the kinesin-like protein Costal2 (Cos2) by Hh. We show that a residue on Cos2, serine 572 (Ser572), is necessary for normal transduction of the Hh signal from the transmembrane protein Smoothened (Smo) to the transcriptional mediator Cubitus interruptus (Ci). This residue is located in the serine/threonine kinase Fused (Fu)-binding domain and is phosphorylated as a consequence of Fu activation. Although Ser572 does not overlap with known Smo- or Ci-binding domains, the expression of a Cos2 variant mimicking constitutive phosphorylation and the use of a specific antibody to phosphorylated Ser572 showed a reduction in the association of phosphorylated Cos2 with Smo and Ci, both in vitro and in vivo. Moreover, Cos2 proteins with an Ala or Asp substitution of Ser572 were impaired in their regulation of Ci activity. We propose that, after activation of Smo, the Fu kinase induces a conformational change in Cos2 that allows the disassembly of the Smo-Fu-Cos2-Ci complex and consequent activation of Hh target genes. This study provides new insight into the mechanistic regulation of the protein complex that mediates Hh signalling and a unique antibody tool for directly monitoring Hh receptor activity in all activated cells.

KEY WORDS: Costal2, Development, *Drosophila*, Hedgehog, Phosphorylation

INTRODUCTION

The evolutionarily conserved proteins of the Hedgehog family (Hh) are signalling molecules that control patterning and organogenesis in metazoans. In *Drosophila*, Hh is necessary for several processes, such as the organisation of the embryonic segments and the patterning of imaginal discs (Ingham and McMahon, 2001). Secreted Hh binds to the receptor Patched (Ptc), a protein with 12 transmembrane domains that acts as a negative effector of Hh signalling (Ingham et al., 1991). It has been proposed that Ptc belongs to a proton gradient-driven transporter family, which could inhibit the transmembrane protein Smoothened (Smo) enzymatically (Taipale et al., 2002; Corcoran and Scott, 2006), and the binding of Hh to Ptc could allow Smo activation. In *Drosophila*, it is known that the activation of Smo leads to its phosphorylation and stabilisation at the plasma membrane (reviewed in Kalderon, 2005), where it then transmits its signal to a multi-protein complex (Robbins et al., 1997; Sisson et al., 1997; Stegman et al., 2000; Monnier et al., 1998). This complex is composed of three major proteins: the kinase Fused (Fu), the kinesin-like protein Costal2 (Cos2) (Sisson et al., 1997; Robbins et al., 1997) and the transcription factor Cubitus interruptus (Ci), which belongs to the Gli protein family and which mediates Hh target gene activation (Alexandre et al., 1996; Methot and Basler, 1999). We and others have shown that the physical interaction between this complex and Smo, presumably via a direct association with Cos2, is necessary for transducing the signal from the membrane (Lum et al., 2003; Ogden et al., 2003; Jia et al., 2003; Ruel et al., 2003). How the complex is regulated and contributes to the regulation of Ci activation, however, remains enigmatic.

It is further known that the Fu-Cos2-Ci complex is associated, again probably via Cos2, with microtubules in an Hh-regulated manner (Robbins et al., 1997; Stegman et al., 2000). We have proposed that this protein complex serves as an anchor to sequester full-length Ci (155 kD, referred to here as Ci155) in the cytoplasm in order to prevent Ci155 nuclear activity in cells not receiving Hh. It has also been recently shown that Cos2 serves as a scaffold protein to bring several kinases in proximity to Ci155 in an Hh-regulated manner (Zhang et al., 2005). These Cos2-associated kinases – protein kinase A (PKA), Shaggy (Sgg) and Casein kinase I (CkIα) – sequentially phosphorylate Ci155 (reviewed in Kalderon, 2005), which will in turn be cleaved by the proteasome (Jia et al., 2005; Smelkinson and Kalderon, 2006; Tian et al., 2005). The truncated form of Ci (75 kD, referred to here as Ci75) binds to DNA and represses the Hh pathway, preventing the transcription of target genes (Aza-Blanc et al., 1997; Methot and Basler, 1999).

The activation of the Hh pathway inhibits the processing of Ci to form Ci75 and induces the accumulation of the full-length form of Ci, Ci155 (Aza-Blanc et al., 1997; Methot and Basler, 1999). The accumulation of Ci155 is insufficient, however, for full-scale Hh target gene activation (Méthot and Basler, 2000; Wang and Holmgren, 2000; Wang et al., 2000), and further steps are needed to reach high levels of signalling. These steps involve the inhibition both of the cytoplasmic anchoring of Ci155 by Suppressor of fused (Sufu) – a protein that binds directly to Ci (Monnier et al., 1998) –

Institute of Signaling, Developmental Biology and Cancer Research, CNRS UMR 6543, Université de Nice-Sophia Antipolis, Parc Valrose, 06108 Nice Cedex 02, France.

*Author for correspondence (e-mail: therond@unice.fr)

Accepted 24 July 2007

and by the Smo-Fu-Cos2 complex (Ohlmeyer and Kalderon, 1998; Méthot and Basler, 2000; Wang and Holmgren, 2000; Wang et al., 2000).

It appears that the only known component of the protein complex necessary to overcome the Ci cytoplasmic anchor is the Fu kinase, because genetic data has shown that Fu represses both Cos2- and Sufu-mediated retention of Ci155 (Methot and Basler, 2000; Wang et al., 2000). The mechanistic regulation of these two proteins by Fu, however, remains to be documented. Cos2 represents one candidate substrate, as suggested in an in vitro study (Nybakken et al., 2002), because it becomes phosphorylated upon Hh signalling and interacts with Fu in a stoichiometric manner (Robbins et al., 1997). Neither in vivo validation of such regulation nor the biological significance of phosphorylation on Cos2, however, has yet been documented.

Genetic data indicate that Cos2 activity has both a positive and a negative role in Hh signalling. The positive role reflects its necessary function in assembling the entire Smo-Fu-Cos2-Ci complex, which is important for relaying the signal from activated Smo to Ci, leading to activation of this protein (Ruel et al., 2003; Lum et al., 2003; Jia et al., 2003; Ogden et al., 2003). In a similar way, the negative role involves tethering Ci outside of the nucleus and promoting the processing of Ci (Zhang et al., 2005). This negative role is revealed in *cos2* loss-of-function mutants, which show intermediate levels of ectopic Hh signalling (Wang et al., 2000; Wang and Holmgren, 2000) thought to be caused by increased levels of Ci155 protein in the cytoplasm that permit Ci to escape cytoplasmic anchoring and activate Hh signalling.

To understand better the functional regulation of the Cos2 protein, we determined the functional role of one of its serine residues in position 572 (Ser572), which is phosphorylated in response to Hh. Using RNA interference (RNAi), creating a kinase-dead version of Fu, and raising a specific antibody that recognizes the phosphorylated form of Cos2, we provide evidence that Ser572 is a substrate of the enzymatic activity of the kinase Fu. We also evaluated the functional role of this serine residue in vitro and in vivo using transgenic variants with alterations to Ser572. We show that, upon phosphorylation of Ser572, association of Cos2 with Smo and Ci is strongly decreased. Transgenic variants mutated on Ser572 were also impaired for Cos2 activity. We propose that this specific Fu-dependent phosphorylation of Cos2 is a pivotal step for the dissociation of Ci from its cytoplasmic anchor in response to Hh.

MATERIALS AND METHODS

Cell culture assays

Drosophila Schneider line-2 (S2) and wing imaginal disc cl8 cells were maintained as described previously (Ruel et al., 2003). *fu* and *cos2* cDNAs and *cos2* fragments were subcloned into pPAC-myc, pPAC-HA or pPAC-V5 *Drosophila* expression vectors. Okadaic treatments of S2 cells were performed with 10 nM for 6 hours. For *ptc* reporter assays, S2 cells treated with or without Hh were transfected with 2 μg *ptc-luciferase*, 2 μg pAct-*lacZ* (in order to normalize for transfection), 0.1 μg of pAct-*ci*, and various amounts of *smo*, *cos2* and *fu* (according to the experiments as indicated in the figure legends). For the experiment in Fig. 3A-D, Hh-expressing cl8 cells were transfected as published (Lum et al., 2003). All experiments were performed in triplicate and luciferase activities normalized with β-galactosidase activity. RNAi treatment, immunoprecipitation and western blot were performed as described previously (Ruel et al., 2003).

Anti-phosphopeptide antibody production

Phospho-specific antibodies directed against phosphorylated Ser572 of Cos2 were produced by immunising rabbits with the following synthetic phosphopeptide: Ser572(P) (P K A V M Q S* Q D R E I E). Reactive antibodies were purified by adsorption on a phosphopeptide (same sequence as above) affinity column. Antibodies were eluted at low pH and dialysed with PBS. These antibodies were further purified by a substraction step on a column containing the non-phosphopeptide of Cos2. From this column, purified antibodies recognising the non-phosphopeptide were also recovered and used for the experiments described in Fig. 4.

Drosophila stock and mutant clone generation

$cos2^{W1}$ FRTG13 is a *cos2* loss-of-function allele recombined with the FRTG13 sequence in order to generate germline clones (glc). Glc were obtained as described previously (Chou and Perrimon, 1996) using the *hsp-70 flp101* flipase. *UAS-cos2-WT*, *UAS-cos2-572A* and *UAS-cos2-572D* transgenic flies were obtained by germline P elements injection. Six to ten independent transgenic lines were obtained for each construct and gave similar results when expressed with various wing disc drivers at different temperatures. Two to three lines, showing similar levels of expression, were further tested for their rescue ability in embryos and in wing discs. Other stocks were obtained from the Bloomington *Drosophila* Stock Center. To generate loss-of-function clones in wing imaginal discs, 24- to 36-hour-old larvae with the following genotype were heat-shocked at 37°C for 1 hour: *y w hs-Flp122;; FRT42D arm lacZ/FRT42D* $cos2^{W1}$*, 71BGal4/UAS cos2-WT-myc* (alternatively UAS *cos2-572A-myc* or UAS *cos2-572D-myc*) and cultured at 18°C until the third instar larval stage.

Cuticle and imaginal disc preparation, immunohistochemistry, immunofluorescence and in situ hybridisation

Cuticle preparation, immunostaining and RNA in situ hybridisation in embryos were performed as previously described (Gallet et al., 2003). Imaginal disc preparation and staining were performed as previously described (Ruel et al., 2003). *wingless* and *rho* antisense RNA probes were made from pBluescript plasmid using T3 polymerase. Alkaline phosphatase-coupled anti-Dig was used at 1/1000 (from Roche manufactory); secondary anti-mouse biotin-conjugated was used at 1/1000 (from Jackson Laboratory). Vector kits were used for peroxidase staining and NBT/BCIP stock solution from Roche manufactory was used for alkaline phosphatase detection. Mouse 4D9 monoclonal anti-Engrailed was used at 1/100, mouse monoclonal 5E11 anti-Ptc at 1/400, rat monoclonal 2A1 anti-Ci at 1/20, mouse monoclonal JB10 anti-Nrt at 1/400, rabbit polyclonal anti-Cos2 (Ruel et al., 2003) at 1/500, rabbit polyclonal anti-Smo at 1/1000, rabbit monoclonal A14 anti-Myc (Santa Cruz) at 1/400, rat monoclonal anti-Myc (Serotec) at 1/400 and monoclonal mouse anti-β-gal at 1:1000 (Promega). Images were captured with a Leica DMR TCS_NT confocal microscope. In Fig. 6, the effect on Ci155 stability of Ser572 mutation in Cos2 was analysed and quantified using the 'plot profile' function of ImageJ software. Co-localisation analyses were performed as described previously (Ruel et al., 2003). Quantitative analyses of Cos2-Ci or Myc-Ci co-localisation images were similarly treated using Adobe Photoshop software and pixels of co-localisation were counted using the histogram function with an intensity threshold defined at 180. Analyses were performed on six to seven independent confocal sections for each genotype.

RESULTS

Development of a specific antibody that recognises an Hh-dependent phosphorylated serine on Cos2, regulated by Fu

It has been shown previously that *Drosophila* Schneider line-2 (S2) and cl8 cells respond to the Hh signal by inducing Cos2 and Fu hyperphosphorylation (Thérond et al., 1996; Robbins et al., 1997; Lum et al., 2003), and that the phosphorylation of Cos2 can be visualised as a change in electrophoretic mobility, or 'shift', of the protein (Robbins et al., 1997; Nybakken et al., 2002) (Fig. 1A). The shift of Cos2 and Fu can be further increased by treatment of S2 cells with the phosphatase inhibitor okadaic acid (OA), suggesting that there are additional phosphorylated sites on Cos2 that were masked by de-phosphorylation in our previous Hh-stimulated cell extracts (Fig. 1A). To test the involvement of Fu, PKA and Sgg kinase activity on Cos2 phosphorylation, we used RNAi. *fu* RNAi treatment

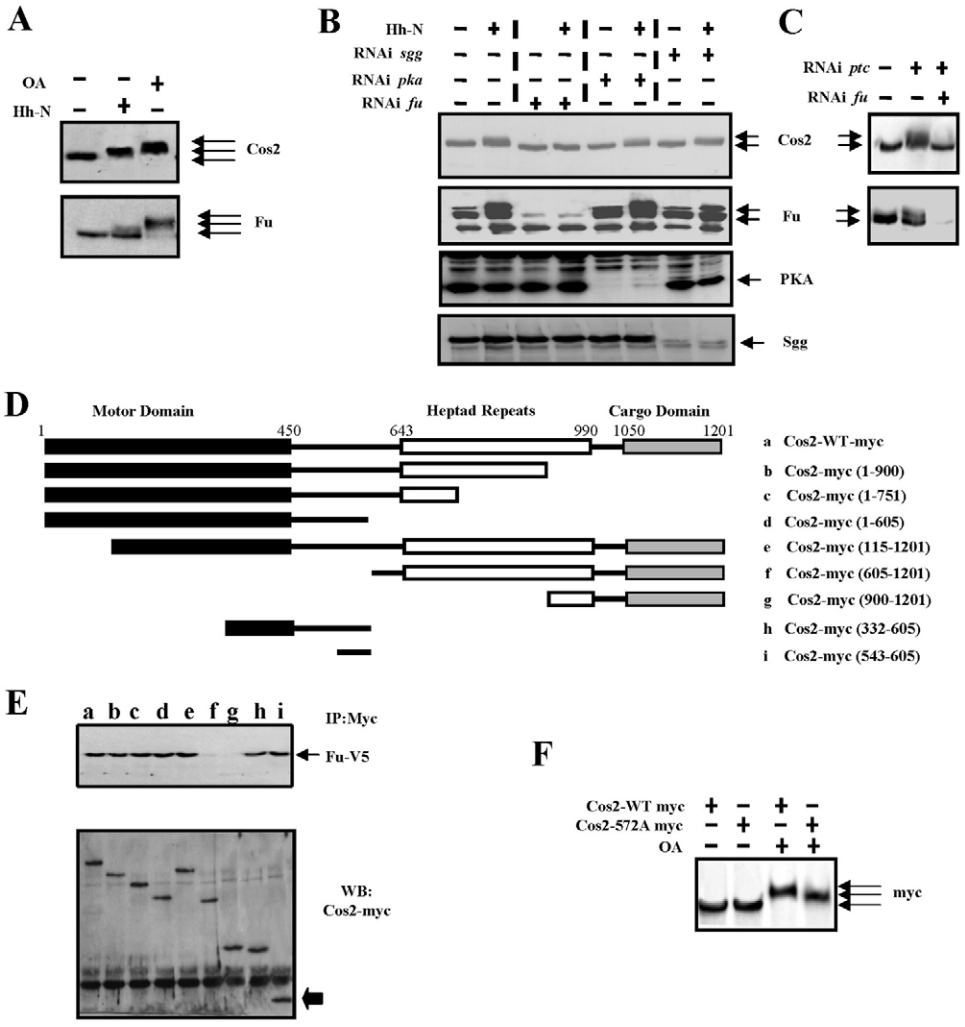

Fig. 1. One of the Hh-dependent Cos2 phosphorylation sites is located within the Fu-binding domain of Cos2. (**A**) Western blot analysis showing the differences in the electrophoretic changes of the Fu and Cos2 proteins in S2 cells treated with Hh-N-conditioned medium or okadaic acid (OA). (**B**) In *fu*-targeted RNAi cells, the Hh-dependent electrophoretic shift of Cos2 is impaired, whereas it is not impaired upon *pka* or *sgg* RNAi treatment. Cellular extracts were subjected to western analysis using Cos2, Fu, Sgg and PKA antibodies. (**C**) *ptc* RNAi induced a Cos2 electrophoretic shift, whereas double RNAi treatment targeting *ptc* and *fu* blocked this shift. (**D**) Structure of wild-type Cos2 protein and Myc-tagged deleted constructs. All constructs contain a Myc tag at the C-terminal end that preserved Cos2 function when expressed in transgenic animals. (**E**) Cells were transfected with *fu-V5* and with different *cos2-myc* constructs (described in D). Immunoprecipitates were analysed for the presence of Fu with an anti-V5 antibody (upper panel) or for the presence of Cos2 with an anti-Myc antibody (lower panel). The large arrow indicates the smallest *cos2-myc* (543-605) construct capable of interacting with the Fu protein. (**F**) S2 cells expressing *cos2-WT-myc* or *cos2-572A-myc* were treated with OA. Arrows indicate the different phosphorylated states of the proteins. WB, western blot.

in Hh-induced cells eliminated the Cos2 electrophoretic mobility change (Fig. 1B), whereas *pka* or *sgg* RNAi treatment had no effect, suggesting that Cos2 phosphorylation is mainly Fu-dependent and that Cos2 is a downstream target of Fu activity upon Hh induction. We confirmed this result via epistatic-relationship studies involving Ptc, Fu and Cos2: the constitutive activation of Cos2 phosphorylation induced by *ptc* RNAi was inhibited by double *ptc fu* RNAi treatment, confirming that the Hh-dependent Cos2 phosphorylation is downstream of Fu activity (Fig. 1C).

We previously showed that Fu and Cos2 are found in the same protein complex, with a similar stoichiometry (Robbins et al., 1997). To precisely identify the Fu-interacting domain on the Cos2 protein, deletion constructs of Cos2 were generated (Fig. 1D) and were tested for their ability to associate with Fu. Whereas all Cos2 constructs that included residues 543 to 605 co-precipitated with Fu, constructs lacking this domain did not (Fig. 1E). Reciprocal immunoprecipitations were also performed and showed similar results (data not shown). Therefore, the Cos2 domain containing residues 543 to 605 is sufficient to form a stable complex with Fu. Importantly, phospho-amino acid analysis of Cos2 co-expressed with Fu in baculovirus-transfected cells revealed that a serine, located in this domain at position 572, can be phosphorylated by Fu in this system (Nybakken et al., 2002). We also confirmed independently that all Cos2 proteins containing residues 543 to 605 responded to OA treatment by a change in electrophoretic mobility, whereas constructs containing only the C-terminal domain, Cos2(605-1201) or Cos2(900-1201), did not (data not shown).

To confirm that phosphorylation of Ser572 depends on Hh induction, a phospho-specific antibody directed against phosphorylated Ser572 of Cos2 was raised. The specificity of the antibody was defined with the Elisa method (data not shown). This antibody revealed a specific Hh-dependent phosphorylated Cos2 isoform that is strongly reduced upon *fu* RNAi treatment (Fig. 2A). However, one can still observe some immunoreactivity, probably due to the presence of a low level of Fu protein, which is not entirely eliminated in most *fu* RNAi experiments. Furthermore, the level of phosphorylated Cos2 increased upon transfection of S2 cells with a Fu (wild type; Fu-WT)-expressing vector and was further enhanced when cells were treated with OA (Fig. 2B, lanes 5 and 6). Moreover, phosphorylated Cos2 was absent in S2 cells transfected with a vector expressing Fu kinase-dead (Fu-KD) (Fig. 2B, lanes 3 and 4). The anti-phosphorylated Ser572 (anti-S572P) Cos2 antibody did not detect a Cos2 variant, Cos2-572A, in which the Ser572 has been replaced with a non-phosphorylatable alanine residue, and which was expressed in S2 cells treated with OA (Fig. 2B, lanes 7 and 8). Finally, the level of phosphorylated Cos2 increased upon transfection of S2 cells with a *smo-WT* or *smo* gain-of-function variant that is constitutively stabilised at the plasma membrane (SmoDDD) (reviewed in Kalderon, 2005) and not with

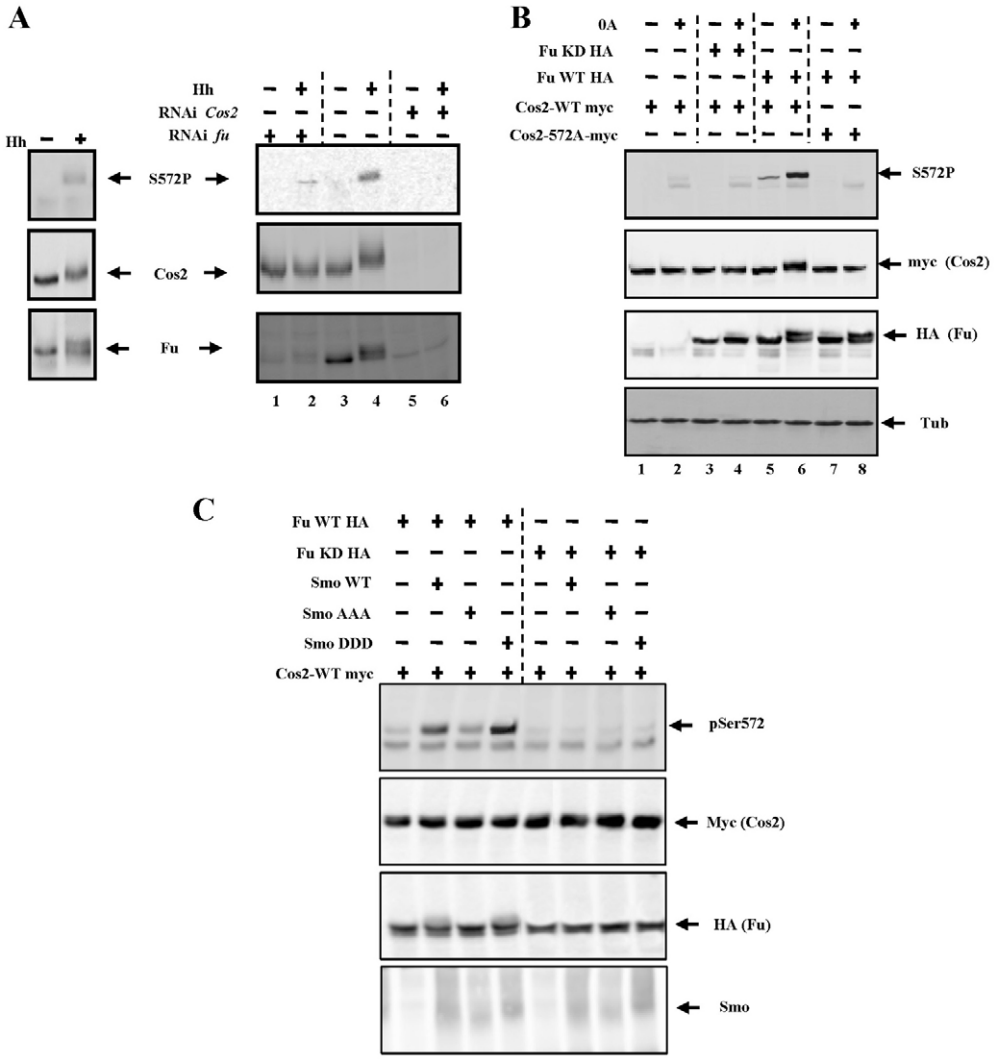

Fig. 2. Specific immunodetection of the Hh-induced phosphorylated form of Cos2 on Ser572. (**A**) On western blot analysis, the anti-S572P antibody specifically detects the Hh-induced phosphorylated form of Cos2 on Ser572. Notice the absence of signal in the non-Hh-expressing cells and the strong decrease in the Hh-expressing cells treated with *fu* RNAi (lane 2 in right panel). (**B**) After transfection with *cos2* and *fu* constructs, S2 cells were treated with okadaic acid (OA) to mimic Hh pathway activation. Notice that phosphorylated Cos2 was absent when cells were transfected with Fu-KD. (**C**) S2 cells were transfected with *cos2-WT-myc*, *fu-WT-HA* and different variants of *smo*. Phosphorylated Cos2 on Ser572 was increased in the presence of the SmoDDD variant but was absent in the presence of SmoAAA or Fu-KD.

a *smo* loss-of-function variant (SmoAAA; Fig. 2C). The SmoDDD-dependent increase of phosphorylated Cos2 is inhibited in the presence of Fu-KD, confirming that phosphorylation at Ser572 is downstream of Smo and Fu activation. All these results suggest that the anti-S572P antibody specifically recognises the Fu-dependent phosphoserine in position 572 of the Cos2 protein and provides us with a unique tool for following the Hh pathway downstream of receptor activation.

Is Ser572 the only site that can be phosphorylated by Hh signalling? We showed that Cos2 shift induced by OA is abrogated when Fu catalytic activity is impaired in S2 cells transfected with *fu*-KD (data not shown), suggesting that shift of Cos2 triggered by OA is physiologically relevant and depends mainly on Fu activity. In order to increase the levels of the phosphorylated Cos2 isoforms and get a global view of all phosphorylated sites on Cos2, S2 cells expressing Cos2-WT or the Cos2-572A variant were treated with OA (Fig. 1F). We observed a reduction in the shift of Cos2-572A relative to Cos2-WT, but the shift was still higher than that displayed by Cos2-WT in non-OA-treated cells (Fig. 1F). This suggests that Cos2 could be phosphorylated not only on S572 but also on other sites. It is important to note that another weaker phosphorylation site on serine at position 931 has been identified in the baculovirus system (Nybakken et al., 2002). However, we did not observe any electrophoretic behaviour differences between the Cos-572A and Cos-572A/931A variants (data not shown), suggesting that Ser931 of Cos2 might not be phosphorylated. Our in vitro analysis did not encourage us to work further on this site; we therefore focused on the physiological relevance of the phosphorylation of Ser572.

Fu-dependent activation of the Hh pathway is linked to phosphorylation of Cos2 on serine 572

We next investigated the role of Cos2 Ser572 in responding to Hh signalling. Recent studies have shown that Cos2 is required positively for the expression of target genes associated with the highest level of Hh signalling (Wang et al., 2000; Wang and Holmgren, 2000), and that Smo can convert Cos2 from a negative factor to a positive one in maximally stimulated cells (Lum et al., 2003). To test the role of Ser572 in this process, we analysed the consequences of serine-to-alanine (S572A) and serine-to-aspartic acid (S572D) alterations on the Smo-dependent conversion of Cos2 activity. To obtain maximal pathway activity, wild-type Hh was co-transfected with different amounts of Smo- and Cos2-expressing vectors. At a fixed level of Smo, a low level of the *cos2-WT* transgene increased the activity of the *ptc-luciferase* reporter gene (*ptc-luc*) (Fig. 3A), as previously shown (Lum et al., 2003). This increase is best observed when the Cos2-WT:Smo expression vector ratio is between 1:10 and 1:100.

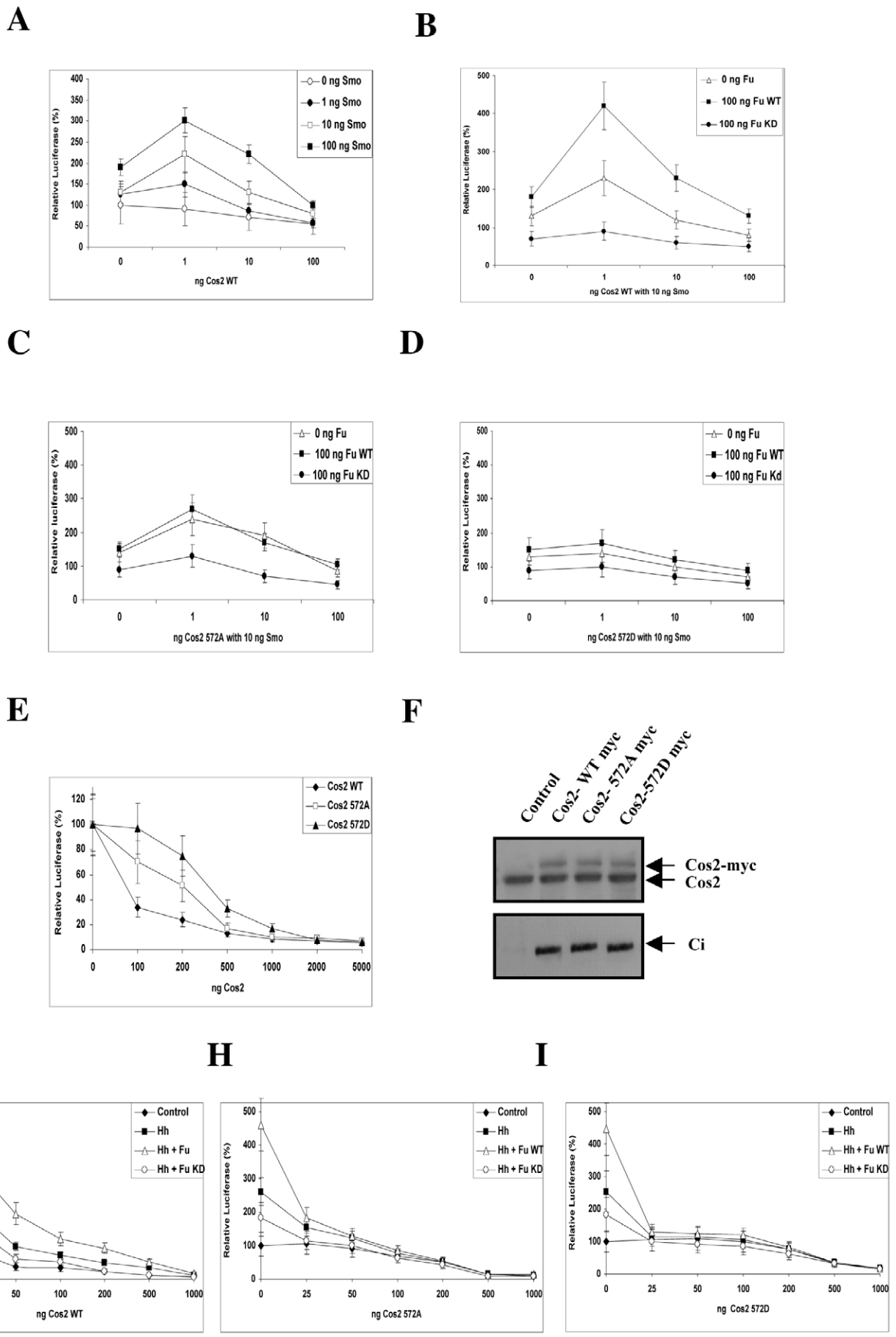

Fig. 3. See next page for legend.

Fig. 3. Activities of Cos2 are affected by mutations in Ser572. (**A**) Hh-expressing cl8 cells were transfected with increasing amounts of *smo* and with different amounts of *cos2-WT*. Ci reporter activity increased in the presence of low levels of transfected *cos2-WT*. (**B-D**) *smo* was transfected at a fixed concentration (10 ng) together with fixed amounts of *fu-WT* or *fu-KD* and with different amounts (0-100 ng) of *cos2-WT* (B), *cos2-572A* (C) or *cos2-572D* (D). Notice that Fu-WT potentiates Ci activity, whereas Fu-KD abolishes the positive effect of Cos2. (**E**) Fixed amounts of *ci* and *ptc-luc* vectors were co-transfected with *cos2* constructs into S2 cells. At high, but not at low, concentrations, the various Cos2 proteins similarly repressed Ci transactivation. (**F**) The levels of the three different Cos2 proteins (500 ng) and the Ci proteins were similar in each pool of transfected cells. (**G-I**) At fixed quantities of *ci* and *ptc-luc* vectors, different amounts of the *cos2-WT* (G), *cos2-572A* (H) and *cos2-572D* (I) constructs were co-transfected into S2 cells, together with fixed amounts of *fu-WT* or *fu-KD* and in the presence or absence (control) of wild-type Hh. In Hh-stimulated cells, the repressive activity of Cos2-WT is regulated by Fu kinase activity, but it is not in the *cos2* mutants in which the phospho-site at position 572 has been affected.

In order to quantify the positive Fu activity in this setup, a Fu-expressing vector was co-transfected with the *smo* and *cos2-WT* constructs (Fig. 3B). In the presence of Fu-WT, a twofold stimulation of reporter gene activity was observed, as compared with cells that were not transfected with the *fu* construct. This effect was due to the catalytic activity of the Fu kinase, because reporter activity was inhibited when the Fu-KD construct, which behaves as a dominant-negative form in vivo (data not shown), was transfected (Fig. 3B).

To determine whether the stimulation of the pathway by Fu is mediated via Cos2 phosphorylation at Ser572, we co-transfected Cos2-572A- and Fu-WT-expressing vectors in this assay. No stimulation of the pathway by Fu was observed, suggesting that the Fu-dependent activation of the pathway relies, at least partially, on phosphorylation of Cos2 Ser572 (Fig. 3C). Interestingly, when a construct expressing a form of Cos2 (Cos2-572D) that mimics a phosphorylated state of the protein was transfected, no activation of the *ptc-luc* reporter was observed, even in the presence of Fu (Fig. 3D), raising the possibility that cycles of phosphorylation and dephosphorylation are important for Cos2 transduction activity. Based on these results, we conclude that phosphorylation of Cos2 on Ser572 is necessary for Fu stimulation of the Hh pathway.

Phospho-Cos2 is absent from the Smo-Fu-Ci complex

We were intrigued by the observation that Cos2-572D had lost its activation capacity. Because binding of Cos2 to Smo is necessary to bridge Smo to Ci (Ruel et al., 2003), it is possible that the lack of Hh signalling activation by Cos2-572D is due to an absence of binding of Cos2-572D to Smo or Ci. We therefore examined the association of Smo and Ci with the different Cos2 mutant forms in cl8 cells. By immunoprecipitation (IP), we observed a weaker association of Smo and Ci with Cos2-572D, as compared with Cos2-WT or Cos2-572A; by contrast, Fu associated similarly with the three tested forms of Cos2 (Fig. 4B, compare lanes 3 and 5 with lane 7). The quantitation of Ci and Smo present in three independent Cos2 IPs confirmed their weak association with Cos572D (Fig. 4C,D).

Using the anti-S572P Cos2 antibody we analysed the interaction of phosphorylated Cos2 with the endogenous proteins of the complex. In non-Hh-treated cl-8 cells, Cos2 protein forms a stable complex with Ci, Smo and Fu (Fig. 4F) (see also Ruel et al., 2003). In Hh-treated cells, Cos2 association with Smo is increased, whereas association with Ci is decreased. Interestingly, when Cos2 IP was performed with the phospho-Cos2 antibody, we observed an association of phosphorylated Cos2 with phosphorylated Fu, but the Smo and Ci proteins were barely detectable in this immunoprecipitate (Fig. 4F).

Because the presence of the phospho-antibody could be interfering with or blocking Fu binding and thereby affecting the stability of the complex, we also performed a similar IP with an antibody against Smo. Although Cos2, Fu and Ci were present in the Smo IP obtained from Hh-treated cell extracts, S572P was barely detectable (Fig. 4G). In another set of experiments, we were also able to precipitate the complex using an anti-Fu antibody. Again, in this IP, the level of Smo was much higher than in the Cos2-S572P IP from Hh-treated cell extracts (Fig. 4G). Importantly, the level of Fu in the two IPs was similar, strongly suggesting that the decreased level of Smo observed in the Cos2-S572P IP was not caused by a decrease in the level of Fu and that the stability of the Fu-Cos2 complex was not affected when we performed IPs with the phospho-Cos2 antibody.

Another possible explanation for the failure of the phospho-specific antibody to pull-down Smo could be that the phospho-epitope is masked within the Smo-Cos2-Fu complex. We therefore developed a new antibody that was raised against the non-phosphorylated Ser572-containing peptide (Fig. 4E, epitopes in green). Thus, we have in hand an antibody that recognises epitopes on a Cos2 peptide that is located within the Fu-binding domain and that could compete with Fu for binding to Cos2. When IPs were performed in parallel with this new antibody, we clearly observed an increased level of Smo in the immunoprecipitate (Fig. 4G). This strongly suggests that the phospho-epitope of Cos2, which is adjacent to the epitope recognised by this second antibody, is not masked in the Smo-Fu-Cos2 complex. From these data, we concluded that, when endogenous Cos2 is phosphorylated on Ser572, it barely associates with either Smo or Ci.

To confirm these biochemical results, we also performed an in vivo analysis of the co-localisation of the Cos2 variants with Smo and Ci. As described previously, the association of Cos2, Smo and Ci can be observed in embryonic ectodermal cells by confocal analysis (Ruel et al., 2003). Interestingly, both Cos2-WT and Cos2-572A co-localised similarly with Ci and with Smo (see Fig. S1D-F′ and I-J′ in the supplementary material), displaying the same frequency as endogenous Cos2 (see Fig. S1B′ and L,M in the supplementary material), whereas Cos2-572D showed a decreased co-localisation with both Ci and Smo (see Fig. S1H,H′,K,K' and L,M). Moreover, Cos2-572D presented a diffused cytoplasmic localisation, whereas the two other constructs displayed an inner-membrane type of localisation (see Fig. S1I-K in the supplementary material).

We further investigated the interaction of Cos2 with Smo by performing immunostaining with the phospho-Cos2 antibody on embryos (Fig. 5). We have previously shown that levels of Cos2 and Fu are downregulated consequent to strong activation of the Hh pathway, probably due to the direct regulation of Cos2 by Smo (Ruel et al., 2003). Conversely, in cells distant to the Hh source, Cos2 and Fu levels were at their highest (Fig. 5D) (see also Ruel et al., 2003). Importantly, we found that Cos2-S572P is at its highest level in Engrailed (En)-positive cells, which produce Hh, and in adjacent cells that respond to Hh (Fig. 5A,C) but is barely detectable in more-distant cells. This pattern is complementary with that obtained with the antibody recognising the anti-heptad repeats of Cos2 (Fig. 5B,D,E). Moreover, although we could detect

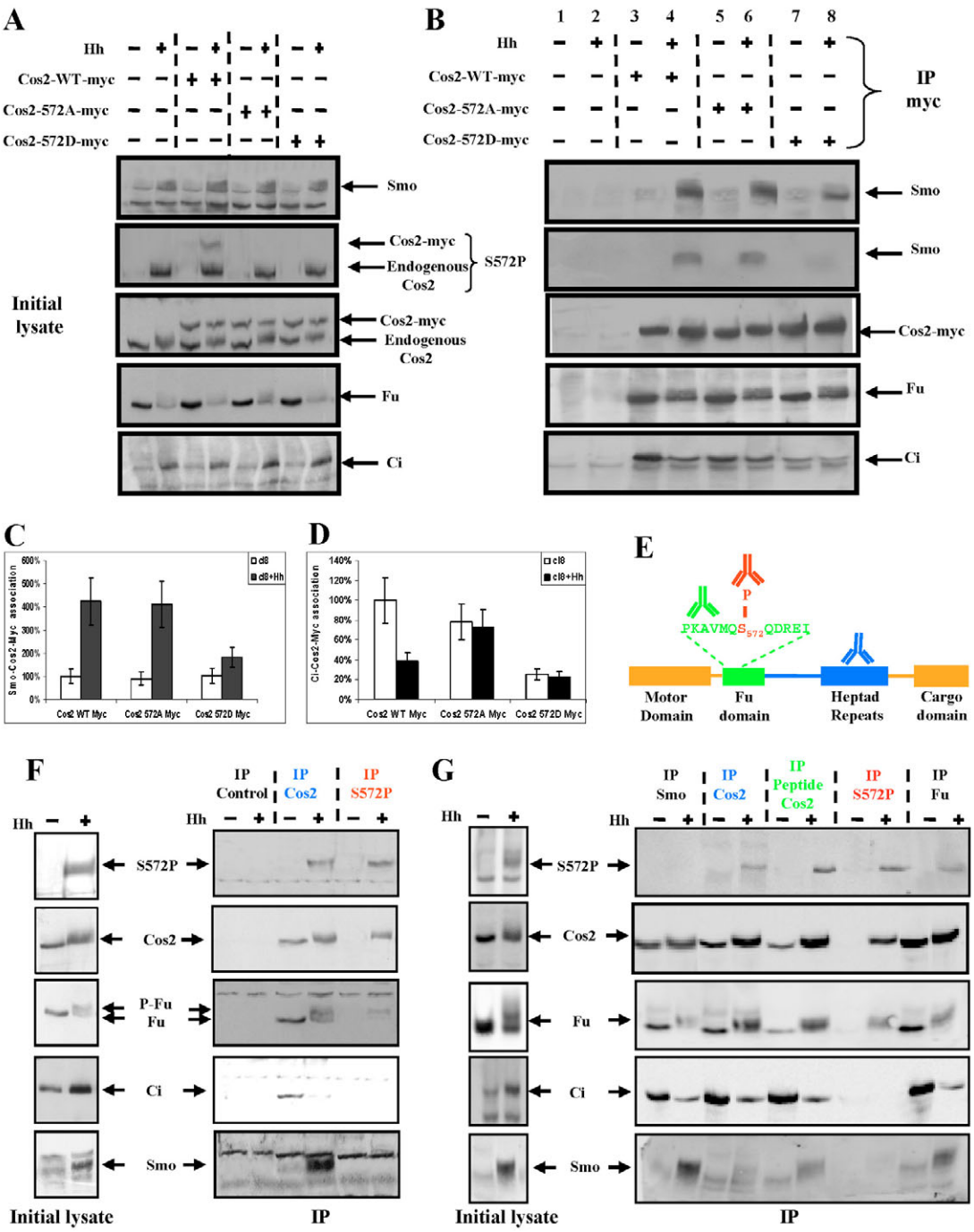

Fig. 4. Phosphorylation of Cos2 on Ser572 strongly reduces its interaction with Smo and Ci. (**A**) Cos2-WT-Myc, Cos2-572A-Myc and Cos2-572D-Myc were revealed with specific antibodies in the initial cl8 cell lysate before immunoprecipitation (IP). Notice that endogenous Smo, Cos2 and Fu proteins were shifted and Ci was stabilised upon Hh treatment. Notice also the presence of a phospho-Ser signal on endogenous Cos2 and on Cos2-WT-Myc in Hh-expressing cells. (**B**) In Cos2 IP, Fu associated similarly with the three different Cos2 variants. The presence of Smo and Ci was strongly reduced in Cos2-572D-Myc IP (lanes 7 and 8) compared with Cos2-WT-Myc and Cos2-572A-Myc IP (lanes 3-6). Two western blots performed from two independent IP experiments are presented for Smo. Notice also that a portion of Ci was dissociated from the protein complex in Hh-treated cells expressing Cos2-WT. This dissociation was less apparent in Cos2-572A-Myc or Cos2-572D-Myc immunoprecipitates. (**C**,**D**) The graphs represent the amount of Smo (C) or Ci (D) associated with the different Cos2 variants after IP, expressed as a percentage relative to the amount of Smo (C) or Ci (D) associated with Cos2-WT in non-Hh-treated cells. The mean of three different experiments is shown. (**E**) Structure of the wild-type Cos2 protein and the relative localisation of the epitopes recognised by the three different Cos2 antibodies used in the IP experiments. (**F**,**G**) Left panels: initial lysates of cl8 cells analysed with specific antibodies. (F) The same extracts were immunoprecipitated with an anti-Cos2 or anti-S572P antibody recognising, respectively, the epitopes shown in blue and in red in E. Under similar conditions, lysates (G) were also submitted to IP with anti-Fu, anti-Smo and three different anti-Cos2 antibodies. Notice the strong decrease in Smo and Ci levels in the IP performed with the S572P antibody. Notice also that phosphorylated Cos2 is absent following IP performed with the anti-Smo antibody, but is present following IP performed with the anti-Fu antibody.

co-localisation of Cos2 with Smo and Ci at the plasma membrane (Ruel et al., 2003), we did not observe overlap of S572P-Cos2 with Ci, Smo or the plasma membrane marker Nrt (Fig. 5F-H). S572P-Cos2 labelling was mainly cytoplasmic as the transgenic Cos2-572D protein. Finally, both transgenic Cos2-WT and Cos2-572A proteins behaved similarly to endogenous wild-type Cos2 protein, with a characteristic periodic pattern of stabilisation (see Fig. S1A,C and E in the supplementary material). By contrast, the level of Cos2-572D did not change (see Fig. S1G in the supplementary material), confirming the lack of Hh regulation and of Smo binding.

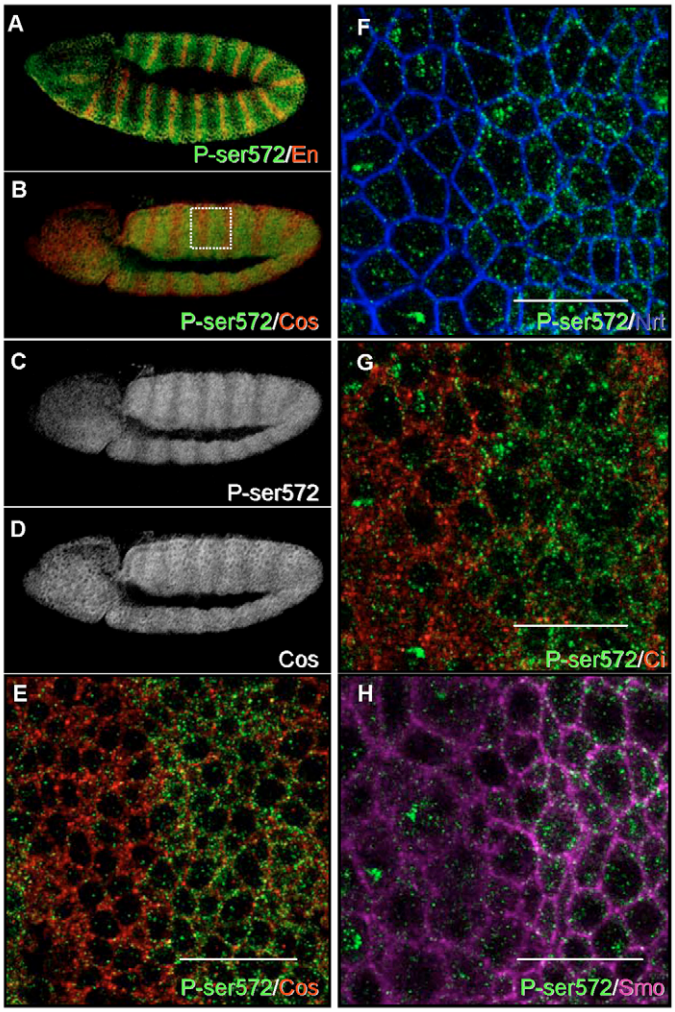

Fig. 5. Activation of the Hh pathway is revealed with the phospho-Cos2 antibody. All pictures are wild-type embryos at stage 10-11. (**A**) En is in red and S572P-Cos2 is revealed in green. Notice that the phospho-Cos2 labelling is only present in Hh-producing cells (in red) and in adjacent cells. (**B**) Staining with the antibody recognising the heptad repeats of Cos2 (red, single channel in **D**); S572P-Cos2 is green (single channel in **C**). (**E**) Magnification (×1260) of one abdominal segment (delimited in by the square in B) showing the complementary Cos2 (red) and S572P Cos2 (green) staining. (**F-H**) Confocal x/y sub-apical sections (magnification ×1890) of one segment from wild-type stage 11 embryos. S572P-Cos2 (F-H) is green, Ci (G) is red, Smo (H) is pink and Nrt (F) is blue. No overlap of S572P-Cos2 with Ci (G), Smo (H) or with the plasma membrane marker Nrt (F) could be detected. S572P-Cos2 labelling is mainly cytoplasmic. White line delimits the Hh-expressing and -receiving cells.

From these data, we can propose that phosphorylation of Ser572 prevents the association of Ci and Smo with Cos2. We propose that the constitutively phosphorylated form of Cos2, represented by Cos2-572D, has lost its activation capacity (as described in Fig. 3D) because it lacks the ability to transfer information from Smo to Ci.

Cos2-572A has decreased sensitivity to the kinase Fu and to Hh signalling activation

If phosphorylation of S572 on Cos2 is necessary for the Hh-dependent dissociation of Cos2 from Ci, one might expect that blocking Ser572 phosphorylation – as in Cos2-572A – would impair the dissociation of Ci from Cos2 in cells induced by Hh and Fu. Accordingly, we found that activation by Hh induces the dissociation of Ci from Cos2-WT, whereas Ci dissociation from Cos2-572A was barely visible upon the same treatment (Fig. 4B, compare lanes 3 and 4 with lanes 5 and 6). This was confirmed in our quantification analysis in Fig. 4D.

To further verify this, we analysed the sensitivity of the repressive activity of Cos2-572A to Hh signalling. The ability of Cos2 to retain Ci outside of the nucleus and thus block its transcriptional activity can be indirectly tested in vitro with the *ptc-luc* reporter gene. Increased quantities of transfected Cos2-WT-expressing vectors repressed *ptc-luc* reporter gene activity in S2 cells (Fig. 3E). Mutant Cos2 proteins showed weaker repressive activity than wild-type Cos2 (except when present at high concentrations) (Fig. 3E), even though the different Cos2 proteins were expressed at similar levels (Fig. 3F). Importantly, Hh treatment counteracted the repressive activity of Cos2-WT on Ci, as evidenced by an increase in *ptc-luc* reporter activity, and this could be further potentiated by Fu-WT or antagonised by Fu-KD (Fig. 3G). By contrast, the repression by Cos2-572A of Ci activity was not sensitive to Hh- or Fu-regulation (Fig. 3H). As expected, Cos2-572D displayed much less repressive activity on Ci as compared with the other Cos2 forms (Fig. 3E) and was not sensitive to Hh signalling activation, probably due to its defects in binding Smo and Ci (Fig. 3I).

Our data suggest that the Ser at position 572 of Cos2 is necessary for the Hh and Fu-controlled modulation of the repression of Ci by Cos2.

Mutations of Ser572 impair Cos2 activity in vivo

To monitor Cos2 mutant activities in vivo, we tested their ability to rescue *cos2* loss-of-function in transgenic animals. During *Drosophila* embryogenesis, Hh is expressed in two rows of cells per segment, under the control of the En transcription factor, and is required for the maintenance of *wingless* (*wg*) and the initiation of *rhomboid* (*rho*) expression (Fig. 6B,C). On the cuticle, the differentiation of denticle types 1 to 4 depends on *rho* activity, whereas naked cell fate depends on *wg* activity (Fig. 6A). Hh loss-of-function abolishes the expression of both *wg* and *rho*, and thus leads to the loss of naked cuticle and denticle identities (Gallet et al., 2003). Conversely, loss-of-function of *cos2* promotes the expansion of *wg* and *rho* expression (Fig. 6E,F), probably due to the loss of Ci cytoplasmic retention or alternatively to the loss of Ci proteolysis, with the consequent transcriptional activation of both targets by Ci. This results in embryos that are covered with naked cuticle, mostly of denticle type 2 (Fig. 6D), comparable to what we have observed following ubiquitous Hh expression (Gallet et al., 2003). Positive Cos2 activity cannot be observed in this setting.

The different Cos2 mutants showed similar levels of expression when expressed in transgenic animals (Fig. 6P,Q). When tested in the *cos2*-null background, we found that the *cos2-WT* transgene

fully rescued the *cos2* cuticular mutant phenotype, as well as rescuing the restricted expression of *wg* and *rho* (Figs 6G-I). Conversely, the *cos2-572A* and *cos2-572D* transgenes only partially rescued the absence of Cos2. Expression of both *wg* and *rho* remained enlarged (Fig. 6K,L,N,O), and the full range of denticle diversity was absent (Fig. 6J,M). Importantly, *cos2-572D* displayed a weaker ability to rescue the phenotype than *cos2-572A*, consistent with the reduced association of Cos2-572D, compared with Cos2-572A, with Ci. These rescue experiments are very sensitive to the level of Cos2 provided by the transgene. Indeed, when raised at 25°C, the embryos displayed a cuticular phenotype that was similar with each transgene (data not shown; i.e. all embryos displayed a reduction in or absence of type 2 denticles). This is probably due to the repression of *rho* expression resulting from the enhanced Ci cytoplasmic retention in all the Cos2 variants due to their increased levels of expression. This result reflects the high sensitivity of Ci activity to small incremental increases in Cos2 levels, as shown in vitro (Fig. 3G,H).

To further evaluate the physiological importance of Cos2 phosphorylation, we also analysed the function of the Cos2 mutants in the wing imaginal disc. In the disc, Ci155 is stabilised by a moderate level of Hh signalling (Fig. 7A). *cos2* loss-of-function clones in the A compartment led to Ci155 stabilisation (Fig. 7B,B′), due to the active role of Cos2 in Ci proteolysis (Zhang et al., 2005). This effect could be rescued by expressing a *cos2-WT* transgene in $cos2^{W1}$ mutant cells, with the help of the *71BGal4* driver (Fig. 7C-C″). Quantification of Ci155 levels showed that the *cos2-WT* transgene reduced the level of Ci155 by 36% relative to the level in $cos2^{W1}$ mutant cells (Fig. 7C; asterisks) located outside of the *71BGal4* expression domain (Fig. 7C). Further, the rescue was almost complete, because the level of Ci155 in the $cos2^{W1}$ clone that was rescued by the *cos2-WT* transgene was only 10% higher than the level in surrounding wild-type cells within the *71BGal4* domain (*n* clones=8).

Performing the rescue experiment with the *cos2-572A* transgene revealed that *cos2-572A* has repressor activity, because the level of Ci155 was reduced by 33% (Fig. 7D-D″; *n* clones=12). However, the

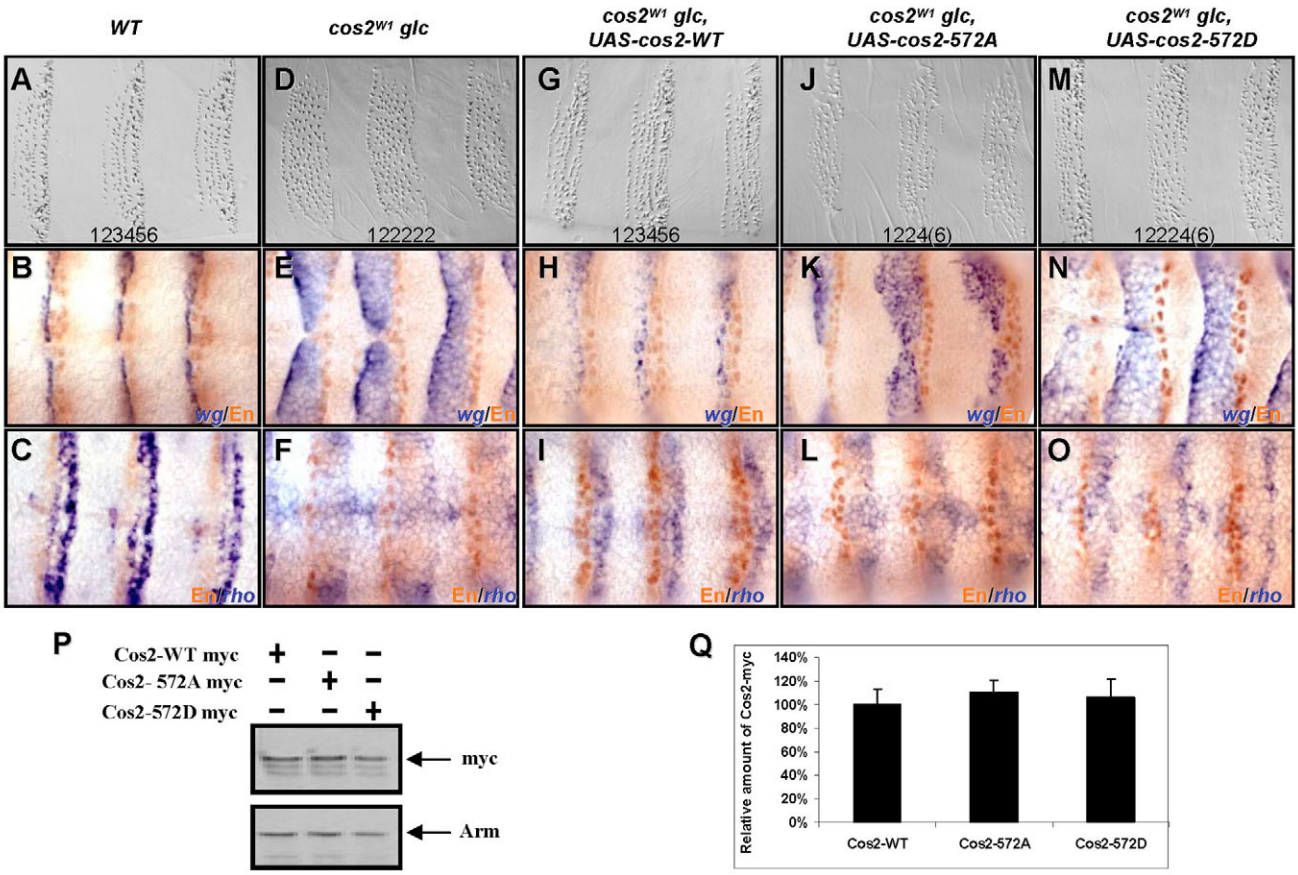

Fig. 6. Cos2-572A and Cos2-572D do not rescue *cos2*-null phenotypes in embryos. (**A-C**) Wild-type embryos. (**D-O**) $cos2^{w1}$ germline clones (glc; D-F) expressing *UAS-cos2-WT* (G-I), *UAS-cos2-572A* (J-L) or *UAS-cos2-572D* (M-O) under the control of the ubiquitous *69BGal4* driver. (A,D,G,J,M) Cuticle views of first instar larva. (Other panels) In blue, mRNA in situ hybridisation for *wg* (B,E,H,K,N) and *rho* (C,F,I,L,O). In brown, immunostaining against En. The wild-type embryo displays an alternating segment pattern of naked cuticle and denticle belts composed of six types of denticles numbered from 1 to 6 (A). In *cos2*-null embryos, an anterior expansion of *wg* (E) and a posterior expansion of *rho* (F) are observed, and only naked cuticle and denticle types 1 and 2 are made (D). Expression of a *cos2-WT* transgene fully rescues the $cos2^{w1}$ glc phenotype defects with restored cuticle pattern and correct Hh target gene expression (G-I). By contrast, the rescue is much weaker with the *cos2-572A* transgene, and is barely observable with *cos2-572D*. Embryos were raised at similar temperatures (18°C). Two to three different transgenic lines were tested for each variant in rescue experiments and showed comparable results. (**P**) Western blot for Cos2-Myc and Arm proteins from embryos expressing *cos2-WT-myc*, *cos2-572A-myc* or *cos2-572D-myc* driven by the *armGal4* driver. (**Q**) Bar graph showing the quantity of Cos2-Myc as analysed by western blot as in P, expressed as a percentage relative to the amount of Arm. The mean of two independent experiments is shown.

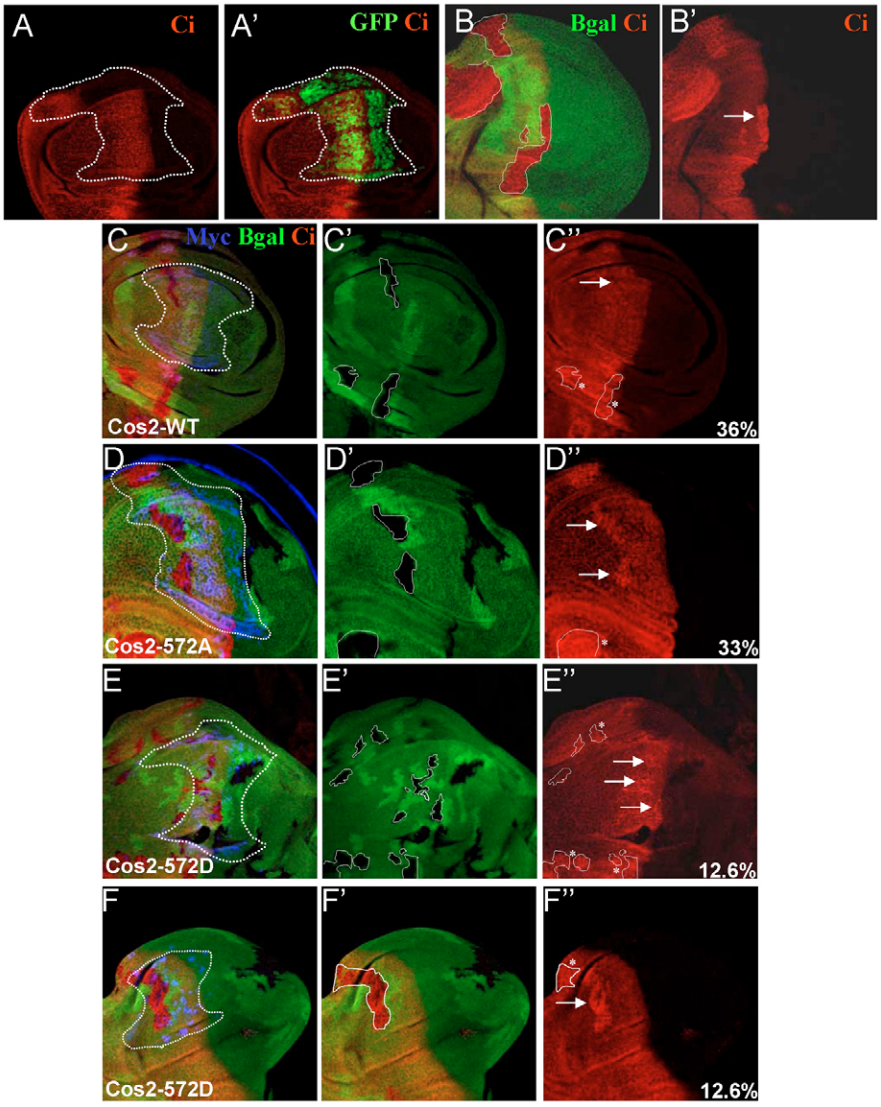

Fig. 7. Phosphorylation of Cos2 on Ser572 impairs its regulation of Ci stability. (A) *71BGal4;UAS-GFP*; (B) *yw,hs-flp; FRT42D cos2^{W1}/FRT42D armlacZ*, (C) *yw,hs-flp; FRT42D cos2^{W1}/FRT42D armlacZ; 71BGAL4/UAS cos2-WT-myc*, (D) *yw,hs-flp; FRT42D cos2^{W1}/FRT42D armlacZ; 71BGAL4/UAS cos2-572A-myc* and (E) *yw,hs-flp; FRT42D cos2^{W1}/FRT42D armlacZ; 71BGAL4/UAS cos2-572D-myc* imaginal discs are stained for Ci (2A1; red), Myc (blue) and β-galactosidase (green), except in A where GFP is in green. (**A**,**A′**) Ci is stabilised in 10-15 cells in the anterior compartment near the anteroposterior (AP) border, as in a wild-type disc. The 71B line drives the expression of Gal4 in a large domain centred in the wing pouch indicated by a broken line. (**B**,**B′**) In *cos2^{W1}* clones, the Ci155 isoform is stabilised, as revealed by the 2A1 antibody (arrow in B′). (**C-F**) Examples of rescue experiments with *UAS-cos2-WT* (C), *UAS-cos2-572A* (D) and *UAS-cos2-572D* (E,F) driven by *71BGal4*. The rescue domain is visualised by Myc staining (encircled). *cos^{WI}* loss-of-function clones are identified by a loss of β-galactosidase staining (**C′-F′**). In **C″-F″**, all the anterior clones outside of the wing pouch are encircled by an unbroken line. The inhibition efficiencies of the wild-type (WT) and mutant *cos2* transgenes were quantified in each disc by comparing Ci155 levels in *cos2^{W1}* clones situated inside the rescue domain (marked by arrows) with clones outside of this domain (asterisk). Inhibition efficiencies were calculated using data obtained from 8-12 different clones for each Cos2 variant and are indicated as percentages in C″-F″. When compared with the surrounding tissues within the driver domain, the Ci level was increased in mutant clones expressing Cos2-WT, Cos2-572A and Cos2-572D by 10.6, 22 and 38.5%, respectively.

rescue by *cos2-572A* was not as efficient as that produced by *cos2-WT*, because the level of Ci155 was increased by 22% in the mutant clones compared with the Ci level in cells surrounding the clone within the driver domain. In contrast to Cos2-WT and Cos2-572A, Cos2-572D expression only weakly inhibited the accumulation of Ci155 induced by the absence of endogenous Cos2 (Fig. 7E-F″; *n* clones=12). Indeed, in this case, the level of Ci155 was only diminished by 12.6%. Also, relative to surrounding tissues, the Ci level was increased by 38.5% in clones expressing Cos-572D. These data suggest that mimicking phosphorylation with the Cos2-572D mutant eliminates the repressive activity of Cos2 on Ci with respect to Ci155 stabilisation, probably due to its inability to associate with Ci.

We also analysed the expression of three targets of Ci – *ptc*, *collier* (*col*) and *en* – in the rescued clones. In the absence of Cos2, *ptc* and *col* were ectopically expressed (see Fig. S3B in the supplementary material, and data not shown), probably due to the disappearance of the Ci-restraining function of Cos2, and endogenous *en* expression was lost in the absence of the positive function of Cos2 (Fig. 8D,D′) (see also Wang et al., 2000; Wang and Holmgren, 2000). Unfortunately, both the endogenous and ectopic expressions of *ptc* and *col* were repressed by all the Cos2 variants (see Figs S2 and S3 in the supplementary material, and data not shown), rendering it impossible to compare the Ci-restraining activities of the different Cos2 variants on *ptc* and *col* expression in the wing disc as we had done in the embryo**.** It is worth noting that this high sensitivity of Ci activity to the level of Cos2 was also illustrated in our in vitro analysis, in which very low levels of Cos2 expression vector (10 to 25 ng) were capable of lowering the activity of Ci (Fig. 3).

When *en* expression was monitored, we found that it was also lost in discs when Cos2-WT expression was driven by *71BGal4* (Fig. 8A,A′). When the level of Cos2 was lowered by removing endogenous Cos2, the transgene failed to rescue *en* expression (Fig. 8E-E″), probably due again to an excessive level of exogenous Cos2 in the wing discs restraining Ci activity and thus masking the positive function of Cos2. Nevertheless, we also tested Cos2-572A and Cos2-572D in this assay. When driven with 71BGal4, none of these variants was able to repress *en* expression as much as did Cos2-WT, confirming their weaker repressive activity on Ci (Fig. 8B-C′). Moreover, *en* expression was not restored in *cos2^{W1}* mutant clones that expressed the Cos2-572D variant (Fig. 8H-H″), consistent with the observation that it was unable to stimulate Hh signalling in vitro (Fig. 3). Importantly, in 40% of the observed cases, Cos2-572A was able to rescue *en* expression in *cos2^{W1}* mutant

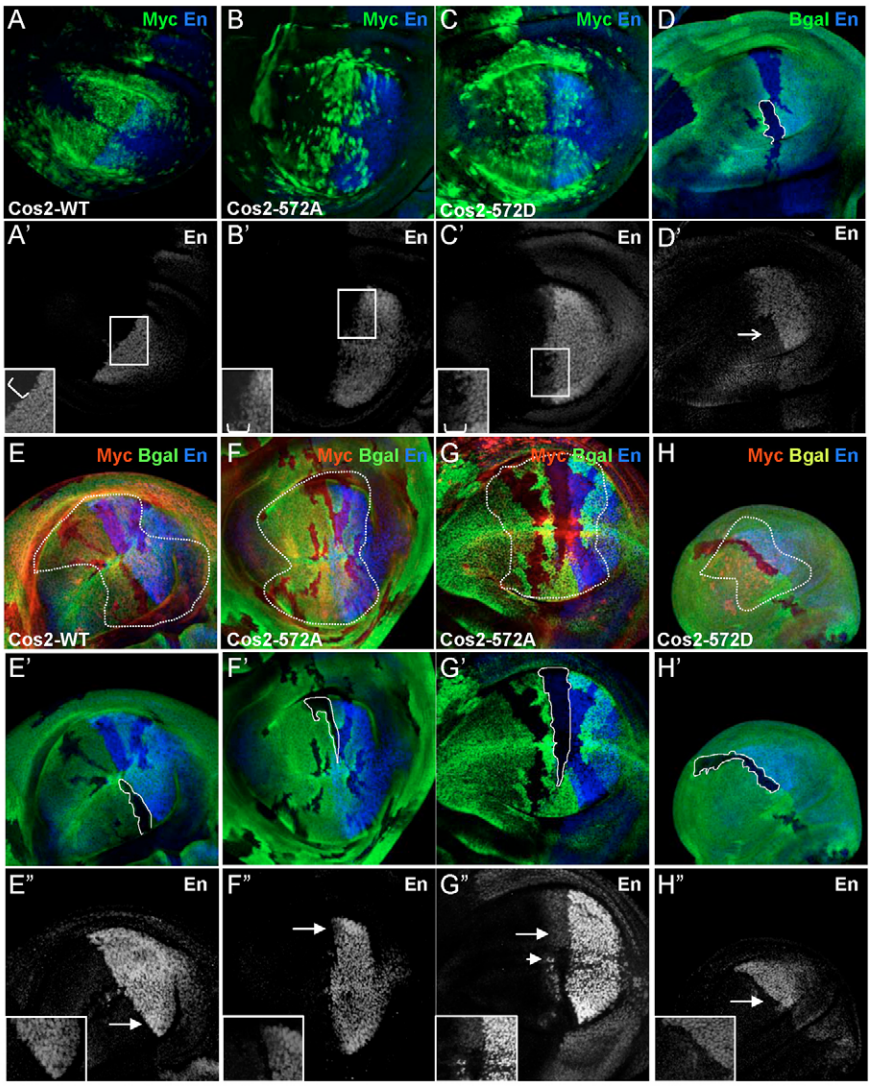

Fig. 8. Phosphorylation of Cos2 on Ser572 is necessary for anterior Engrailed expression. (**A**) *71BGAL4/UAS cos2-WT-myc*, (**B**) *71BGAL4/UAS cos2-572A-myc*, (**C**) *71BGAL4/UAS cos2-572D-myc* and (**D**) *yw,hs-flp; FRT42D cos2^{W1}/FRT42D armlacZ* imaginal discs are stained for En (4D9) in blue and Myc in green, except in D,D′ in which β-gal is in green. (**A′-D′**) En is in white and an enlargement of the squared region is shown; the bracket indicates the anterior region at the anteroposterior (AP) boundary. (**E**,**E′**) *yw,hs-flp; FRT42D cos2^{W1}/FRT42D armlacZ;ac71BGAL4/UAS cos2-WT-myc*, (**F-G′**) *yw,hs-flp; FRT42D cos2^{W1}/FRT42D armlacZ; 71BGAL4/ UAS cos2-572A-myc* and (**H**,**H′**) *yw,hs-flp; FRT42D cos2^{W1}/FRT42D armlacZ; 71BGAL4/UAS cos2-572D-myc* imaginal discs are stained for Myc (red), β-gal (green) and En (blue). (**E″-H″**) En is in white and enlargements of the *cos2^{W1}* clones pointed to by an arrow are shown. (A) In the anterior region, Cos2-WT transgene expression (18°C) is sufficient to strongly inhibit the endogenous expression of En. (B) The two mutant Cos2 variants are less efficient, because *en* expression is only slightly reduced. (D) Cos2 is necessary for the high level of Hh signalling, because En expression is lost (arrow in D′) in anterior *cos2^{W1}* loss-of-function clones situated at the AP boundary. (E-H) En expression in anterior clones situated inside the 71B domain at the AP boundary was observed in different discs from distinct experiments (*n* clones=11 to 15). The rescue domain is visualised by Myc staining and encircled in E-H. *cos2^{WI}* loss-of-function clones are identified by loss of β-gal staining, and anterior clones near the AP boundary are encircled by an unbroken line (E′-H′), or arrows (E″-H″). En expression is absent in *cos2^{W1}* loss-of-function clones expressing the *cos2-WT* and *cos2-572D* transgenes. Expression of the *cos2-572A* transgene gave similar results in 60% of the discs (F-F″), but in the other 40%, a low level of En was detected in *cos2^{W1}* loss-of-function clones in which Cos2-572A was expressed at a low level (G-G″). Notice that the level of En is much higher in the few anterior cells outside of the *cos2* mutant clone (arrowhead in G″). Notice also that some cells in the *cos2^{W1}* clones (G″) showed no En expression due to the higher expression of the transgene in these cells.

clones (Fig. 8G-G″). Interestingly, the level of rescued *en* expression was not as high as in wild-type anterior cells, consistent with our in vitro results showing that Ser572 is necessary to allow the full activation of the pathway (Fig. 3).

DISCUSSION

Our data show that phosphorylation of Cos2 residue Ser572 is necessary for the full activation of Hh signalling, and that this phosphorylation is dependent on the kinase Fu. It is likely that Fu directly phosphorylates Cos2 on Ser572, but we were unable to purify an activated Fu kinase to confirm this. The phosphorylation of this residue strongly decreased the association of Cos2 with both Ci and Smo, an important step in the regulation of the cytoplasmic anchoring of Ci. By contrast, Cos2-572A, a Cos2 mutant that cannot be phosphorylated at Ser 572, remained associated with Smo and Ci but was much less sensitive to Hh regulation; this is because both its restraining activity on Ci and its association with Ci were only minimally sensitive to the presence of Fu and to the activation of Hh signalling.

Phosphorylation of Ser572 of Cos2 induces the partial disassembly of the protein complex

Our data show that Cos2 phosphorylated on Ser572 does not bind Smo. However, previous studies have shown that Cos2 is phosphorylated and is pulled down by Smo in response to Hh stimulation (Ruel et al., 2003; Lum et al., 2003). How can we reconcile these data? First, it is possible that not all Cos2 proteins that bind to Smo are phosphorylated. Indeed, we observed that only a limited fraction of Cos2 and Fu are sensitive to Hh activation. This is clearly observed with Fu (only 50% of the protein undergoes an electromobility shift upon Hh activation), but is more difficult to quantify with Cos2 because of its very small and diffused electromobility shift. Nevertheless, if Cos2 behaves similarly to Fu, it would mean that 50% of the total Cos2 (corresponding to the non-modified protein in Hh-treated cells) should be able to bring enough Smo down to be detectable in immunoprecipitates. Second, it is possible that Smo still binds to phosphorylated Cos2 on Ser572, but with much less affinity. Third, phosphorylation on Ser572 is not responsible for all Cos2 mobility shift, because Cos2-572A still

shifts upon OA treatment, suggesting that other phosphorylated sites are present. Therefore, some phosphorylated isoforms that are not phosphorylated on Ser572 might also be associated with Smo. It is thus possible that our study has only revealed one of a series of sequential phosphorylation events on Cos2 that ultimately lead to the complete dissociation of Cos2 from Smo. Finally, it is worth mentioning that more Smo is present in the Cos2 IP from Hh-treated cells than in non-Hh treated cells (Ruel et al., 2003; Lum et al., 2003). To us, this simply reflects an increased level of Smo resulting from Hh signalling activation, and not the Hh-dependent regulation of the efficiency of the interaction of Smo with Cos2.

Mechanistic regulation of the protein complex that mediates Hh signalling

The role of the Cos2 protein in the complex is to serve as a platform to allow both positive and negative regulators to be brought into close proximity with Smo and Ci. Thus, the role of Cos2 in transmitting a response can be masked by the role of Cos2 in limiting pathway activity in the absence of Hh. At low concentrations, it is able to stimulate Hh reporter activity in vitro and *en* expression in vivo. But in Cos2-572A-expressing cells, *en* expression was lower than in wild-type discs (Fig. 8), and the in vitro stimulation of Hh signalling could not be potentiated by Fu activity (Fig. 3C). Moreover, the restraining activity of Cos2-572A on Ci could not be counteracted by Hh or Fu in vitro (Fig. 3H). Therefore, we propose that the Ser572 to Ala substitution on Cos2 rendered Cos2 less sensitive to Hh and Fu regulation. Because Cos2-572A still binds to its partners, it could bring Fu into proximity with its other targets. Indeed, it is likely that Fu activation leads not only to the direct phosphorylation of Cos2 but also to direct changes in Ci and/or other partners, such as Sufu. This explains why Cos2-572A is still able to stimulate Hh signalling, albeit not to its highest level.

From the Cos2-572A results, one could wonder why Cos2-572D did not constitutively activate the pathway. Because the Cos2-572D form is in a 'frozen' state compared with the wild-type form, cycles of phosphorylation/dephosphorylation are blocked and thus Cos-572D cannot participate in the Hh complex signalling anymore. Our data show that constitutively phosphorylated Cos2 and endogenous phospho-Cos2 are bound to Fu but are dissociated from Smo and Ci. Therefore, Fu bound to phosphorylated Cos2 would be absent from the complex, preventing the release of all the cytoplasmic anchors from Ci.

Because the Cos2 Ser572 residue is not part of the Ci- or Smo-binding domains (Ruel et al., 2003; Lum et al., 2003; Ogden et al., 2003), but phosphorylation of this site nevertheless leads to the dissociation of these two proteins from Cos2, we propose that the Fu-mediated modification of Cos2 induces the protein to undergo a conformational change that leads to the disassembly of the complex. The disassembly is partial because phosphorylated Cos2 and Fu are still associated. Interestingly, it has been proposed that the binding of Cos2, Sufu and Fu to Ci masks a nuclear localisation site on Ci (Ci-NLS) (Wang and Jiang, 2004). We propose a conformational change that supports this idea: that disassembly of the complex is necessary to expose the Ci-NLS and for consequent nuclear translocation.

We thank A. LeBivic, R. Holmgren, P. Ingham, M. Bourouis, K. Ho, M. Scott, D. Kalderon and P. Beachy for providing fly stocks and reagents. We thank R. Rodriguez for panel B,B′ in supplementary material Fig. S2. We are thankful for the editing skills of P. Follette, K. Ayers and G. D'Angelo. This work was supported by grants from Fondation de France and Ligue National Contre le Cancer 'équipe labelisée 2005' to P.P.T.

Supplementary material

Supplementary material for this article is available at http://dev.biologists.org/cgi/content/full/134/20/3677/DC1

References

Alexandre, C., Jacinto, A. and Ingham, P. W. (1996). Transcriptional activation of hedgehog target genes in Drosophila is mediated directly by the cubitus interruptus protein, a member of the GLI family of zinc finger DNA-binding proteins. *Genes Dev.* **10**, 2003-2013.

Aza-Blanc, P., Ramirez, W. F., Laget, M. P., Schwartz, C. and Kornberg, T. B. (1997). Proteolysis that is inhibited by hedgehog targets Cubitus interruptus protein to the nucleus and converts it to a repressor. *Cell* **89**, 1043-1053.

Chou, T. B. and Perrimon, N. (1996). The autosomal FLP-DFS technique for generating germline mosaics in Drosophila melanogaster. *Genetics* **144**, 1673-1679.

Corcoran, R. B. and Scott, M. P. (2006). Oxysterols stimulate Sonic hedgehog signal transduction and proliferation of medulloblastoma cells. *Proc. Natl. Acad. Sci. USA* **103**, 8408-8413.

Gallet, A., Rodriguez, R., Ruel, L. and Thérond, P. P. (2003). Cholesterol modification of Hedgehog is required for trafficking and movement, revealing an asymmetric cellular response to Hedgehog. *Dev. Cell* **4**, 191-204.

Ingham, P. W. and McMahon, A. P. (2001). Hedgehog signalling in animal development: paradigms and principles. *Genes Dev.* **15**, 3059-3087.

Ingham, P. W., Taylor, A. M. and Nakano, Y. (1991). Role of the Drosophila patched gene in positional signalling. *Nature* **353**, 184-187.

Jia, J., Tong, C. and Jiang, J. (2003). Smoothened transduces Hedgehog signal by physically interacting with Costal-2/Fused complex through its C-terminal tail. *Genes Dev.* **17**, 2709-2720.

Jia, J., Zhang, L., Zhang, Q., Tong, C., Wang, B., Hou, F., Amanai, K. and Jiang, J. (2005). Phosphorylation by double-time/CKIepsilon and CKIalpha targets cubitus interruptus for Slimb/beta-TRCP-mediated proteolytic processing. *Dev. Cell* **9**, 819-830.

Kalderon, D. (2005). The mechanism of hedgehog signal transduction. *Biochem. Soc. Trans.* **33**, 1509-1512.

Lum, L., Zhang, C., Oh, S., Mann, R. K., von Kessler, D. P., Taipale, J., Weis-Garcia, F., Gong, R., Wang, B. and Beachy, P. A. (2003). Hedgehog signal transduction via Smoothened association with a cytoplasmic scafforded by the atypical kinesin, Costal-2. *Mol. Cell* **12**, 1261-1274.

Methot, N. and Basler, K. (1999). Hedgehog controls limb development by regulating the activities of distinct transcriptional activator and repressor forms of Cubitus interruptus. *Cell* **96**, 819-831.

Methot, N. and Basler, K. (2000). Suppressor of fused opposes hedgehog signal transduction by impeding nuclear accumulation of the activator form of Cubitus interruptus. *Development* **127**, 4001-4010.

Monnier, V., Dussillol, F., Alves, G., Lamour, I. C. and Plessis, A. (1998). Suppressor of fused links fused and Cubitus interruptus on the Hedgehog signaling pathway. *Curr. Biol.* **8**, 583-586.

Nybakken, K. E., Turck, C. W., Robbins, D. J. and Bishop, J. M. (2002). Hedgehog-stimulated phosphorylation of the kinesin-related protein Costal2 is mediated by the serine/threonine kinase Fused. *J. Biol. Chem.* **277**, 24638-24647.

Ogden, S. K., Ascano M., Jr, Stegman, M. A., Suber, L. M., Hooper, J. E. and Robbins, D. J. (2003). Identification of a functional interaction between the transmembrane protein Smoothened and the kinesin-related protein Costal2. *Curr. Biol.* **13**, 1998-2003.

Ohlmeyer, J. T. and Kalderon, D. (1998). Hedgehog stimulates maturation of Cubitus interruptus into a labile transcriptional activator. *Nature* **396**, 749-752.

Robbins, D. J., Nybakken, K. E., Kobayashi, R., Sisson, J. C., Bishop, J. M. and Thérond, P. P. (1997). Hedgehog elicits signal transduction by means of a large complex containing the kinesin-related protein costal2. *Cell* **90**, 225-234.

Ruel, L., Rodriguez, R., Gallet, A., Lavenant-Staccini, L. and Thérond, P. P. (2003). Stability and association of Smoothened, Costal-2 and Fused with Cubitus interruptus are regulated by Hedgehog. *Nat. Cell Biol.* **5**, 907-913.

Sisson, J. C., Ho, K. S., Suyama, K. and Scott, M. P. (1997). Costal 2, a novel kinesin-related protein in the Hedgehog signaling pathway. *Cell* **90**, 235-245.

Smelkinson, M. G. and Kalderon, D. (2006). Processing of the Drosophila hedgehog signalling effector Ci-155 to the repressor Ci-75 is mediated by direct binding to the SCF component Slimb. *Curr. Biol.* **16**, 110-116.

Stegman, M. A., Vallance, J. E., Elangovan, G., Sosinski, J., Cheng, Y. and Robbins, D. J. (2000). Identification of a tetrameric Hedgehog signaling complex. *J. Biol. Chem.* **275**, 21809-21812.

Taipale, J., Cooper, M. K., Maiti, T. and Beachy, P. A. (2002). Patched acts catalytically to suppress the activity of Smoothened. *Nature* **418**, 892-897.

Thérond, P. P., Knight, J. D., Kornberg, T. B. and Bishop, J. M. (1996). Phosphorylation of fused protein kinase in response to signaling from Hedgehog. *Proc. Natl. Acad. Sci. USA* **93**, 4224-4228.

Tian, L., Holmgren, R. A. and Matouschek, A. (2005). A conserved processing mechanism regulates the activity of transcription factors Cubitus interruptus and NF-KappaB. *Nat. Struct. Mol. Biol.* **12**, 1045-1053.

Wang, G. and Jiang, J. (2004). Multiple Cos2/Ci interactions regulate Ci subcellular localization through microtubule dependent and independent mechanisms. *Dev. Biol.* **268**, 493-505.

Wang, G., Amanai, K., Wang, B. and Jiang, J. (2000). Interactions with Costal2 and suppressor of fused regulate nuclear translocation and activity of Cubitus interruptus. *Genes Dev.* **14**, 2893-2905.

Wang, Q. T. and Holmgren, R. A (2000). Nuclear import of Cubitus interruptus is regulated by Hedgehog via a mechanism distinct from Ci stabilization and Ci activation. *Development* **127**, 3131-3139.

Zhang, W., Zhao, Y., Tong, C., Wang, G., Wang, B., Jia, J. and Jiang, J. (2005). Hedgehog-regulated Costal2-kinase complexes control phosphorylation and proteolytic processing of Cubitus interruptus. *Dev. Cell* **8**, 267-278.